2014 American Control Conference (ACC)
June 4-6, 2014. Portland, Oregon, USA

Aggregate Modeling and Control of Plug-in Electric Vehicles for Renewable Power Tracking

Behrouz Ebrahimi*, Javad Mohammadpour

Abstract— **A robust strategy is proposed in this paper to control the aggregate charging power of plug-in electric vehicles (PEVs). The charging flexibility of PEVs provides the intermittent renewable power sources with control authority to cope with load fluctuations caused by the variation of grid-connected PEVs population and their instantaneous power demand. In this paper, we consider an aggregate model of PEVs power in the form of a partial differential equation (PDE). A sliding mode control is then developed for the derived PDE load model with no discretization in the spatial domain. The developed sliding mode controller operates on the real-time measurable imbalance between source and demand power. To evaluate the closed-loop response and demonstrate the controller's robustness against PEVs population variations, a Monte Carlo simulation is performed for real driving conditions and using renewable power data.**

I. Introduction

The charging flexibility of plug-in electric vehicles (PEVs) provides the power grid with some degree of control authority over load variation of grid-connected PEVs population. However, the uncertainties associated with the available renewable power and the number of PEVs connected to the grid complicate the process of distributing the renewable power among the grid-connected PEVs. There have been several studies to examine both negative and positive impacts of PEVs on the power grid (see e.g., [1], [2], [3]). The negative aspect has mainly been the effect of the additional load by PEVs on the grid and overstretching it for large population of PEVs connected to the grid. On the other hand, the PEVs' charging flexibility is deemed beneficial, because it enables the grid to reduce the strain and accommodates the renewable power to a greater extent [4].

From the controls point of view, the interplay between PEVs and the power grid has been considered generally as the proper grid power distribution among the grid-connected PEVs. In the past decade, various modeling and control approaches have been developed for aggregate PEVs power demand [1], [5], [6]. The modeling efforts have primarily considered assigning an average value for the PEVs' maximum charging power, which is presumably independent of the number of PEVs. A great effort has been recently made by Bashash and Fathy to develop a control-oriented model for grid-connected PEVs aggregate load demand using partial differential equations (PDEs) [7].

B. Ebrahimi was with College of Engineering, University of Georgia, Athens, GA 30602, USA. He is now with Department of Mechanical Engineering, University of Houston, Houston, TX 77204, USA (corresponding author: bebrahimi@uh.edu).

J. Mohammadpour is with College of Engineering, University of Georgia, Athens, GA 30602, USA (javadm@uga.edu).

Control-oriented aggregate load PDE modeling has gained tremendous interest to model a large number of homogeneous lumped systems defined individually by a similar ordinary differential equations (ODEs). They have been primarily introduced for thermostatically controlled load systems based on load transport notions [5]. Aggregate PDE modeling has been further developed for heterogeneous populations to address the inhomogeneity of lumped ODE systems [8]. A novel transport-based bilinear advection PDE has been developed for PEVs aggregate load modeling, where the PEVs have been postulated as dynamic loads diffusing from a lower state-of-charge (SOC) to a higher SOC [7]. Hence, the proposed PDE has been constructed on the storage level and time as the independent variables and the control input explicitly configured to control the propagation speed of the advection hyperbolic PDE. The storage interval has been discretized into equal segments and finite-difference approaches have been employed to represent the system in a form appropriate for control design purpose. In this paper, we will employ the same bilinear advection PDE and propose a control system directly using the PDE model rather than discretizing it to track the reference power profile.

In this paper, we adopt sliding mode theory to design a robust feedback control system for the PEVs power demand control. It is assumed that the grid provides the control system with real-time supply/demand error signal. A Monte Carlo simulation with real data is conducted to demonstrate the effectiveness of the proposed control approach in tracking the sluggish renewable reference power and in dealing with the population variations of the grid-connected PEVs. The aggregate PDE model developed in this paper was recently developed in [7] using a different approach. The approach we take here follows a more systematic procedure. In terms of the control design method, the control strategy proposed in this paper directly employs the PDE model representation, while the control in [7] uses a discretized form of the PDE representation.

The paper is organized as follows. Section II formulates the aggregate power PDE representation. In Section III, we present a PDE-based control architecture for charging power of PEVs. Monte Carlo simulation results are presented and discussed in Section IV and concluding remarks are provided in Section V.

II. Problem Formulation

The aim of this work is to develop a control strategy in order to adjust the charging rate of PEVs. To this purpose, we

978-1-4799-3274-0/$31.00 ©2014 AACC

first consider the transport-based partial differential equation (PDE) modelling of aggregate load of PEVs. Let D be a fixed spatial domain of the collective PEVs to be charged, and denote its boundary by ∂D. By using energy conservation law, we write the change in the energy stored in D between time instants t and $t+\Delta t$ as

$$\int_D [Q(x,t+\Delta t)-Q(x,t)]dV = \int_t^{t+\Delta t}\int_D \omega(x,t)dV\,dt - \int_t^{t+\Delta t}\int_{\partial D}\mathbf{F}(x,t).\mathbf{n}dS\,dt, \tag{1}$$

where $Q(x,t)$ is the PEVs concentration, x is the energy storage level, $\omega(x,t)$ is the rate of connected/disconnected PEVs to the grid, $\mathbf{F}(x,t)$ is the load flux through the boundary, dV and dS are space and surface integration elements, respectively, and $\mathbf{n}$ is a unit vector pointing outward normal to ∂D. By approximating the t integrals using the mean value theorem, dividing both sides of (1) by Δt, and taking its limit when $\Delta t \to 0$, Eq. (1) can be rewritten as

$$\int_D \frac{\partial Q(x,t)}{\partial t}dV = \int_D \omega(x,t)dV - \int_{\partial D}\mathbf{F}(x,t).\mathbf{n}dS. \tag{2}$$

By using Gauss theorem to convert the surface integral into a volume integral, Eq. (2) can be expressed in the following form

$$\int_D \Big[\frac{\partial Q(x,t)}{\partial t} - \omega(x,t) + \nabla.\mathbf{F}(x,t)\Big]\mathrm{d}V = 0, \tag{3}$$

where $\nabla.$ denotes the divergence operator and depends on the spatial variable x, i.e., storage level. Now, let the load flux into the domain be

$$F(x,t) = P_{\max}u(t)Q(x,t), \tag{4}$$

where $P_{\max}$ is the maximum charging power of individual PEVs and $u(t)$ is the control input dictated by the grid. Hence, the third term in (3) is simplified to $\nabla.\mathbf{F}(x,t) = P_{\max}u(t)\frac{\partial Q(x,t)}{\partial x}$ and consequently, Eq. (3) expressed as

$$\int_D \Big[\frac{\partial Q(x,t)}{\partial t} - \omega(x,t) + P_{\max}u(t)\frac{\partial Q(x,t)}{\partial x}\Big]\mathrm{d}V = 0. \tag{5}$$

We use the following lemma to further simplify the integral equation (5).

Lemma: *Let* $h(x,t) = \frac{\partial Q(x,t)}{\partial t} - \omega(x,t) + P_{max}u(t)\frac{\partial Q(x,t)}{\partial x}$ *be a continuous function satisfying Eq. (5), i.e.,* $\int_D h(x,t)dV = 0$*, for every domain* D*. Then* $h(x,t) \equiv 0$.

Proof: Let us assume that there exists a point $p = (x_0, t_0)$ where $h(p) \neq 0$. Without loss of generality one can assume $h(p) > 0$. Due to the continuity of $h(x,t)$, there exists a domain D_0 which contains p and ϵ where $h > \epsilon > 0$. Hence, $\int_{D_0} hdV > \epsilon Vol(D_0) > 0$ which is in contradiction with the lemma's assumption. This concludes that $h(x,t) = 0$ and hence proves the lemma. □

Based on preceding lemma, Eq. (5) can now be expressed in the following PDE form

$$\frac{\partial Q(x,t)}{\partial t} - \omega(x,t) + P_{\max}u(t)\frac{\partial Q(x,t)}{\partial x} = 0. \tag{6}$$

Eq. (5) is a PDE that represents the aggregate power of PEVs and has been derived in a different manner in [7]. It is assumed that the input and output flows are fully contained in the disturbance term $\omega(x,t)$ and, hence, the boundary conditions are considered as

$$Q(x_{\max},t) = 0, Q(x_{\min},t) = 0. \tag{7}$$

The systems represented by (6) is a first-order bilinear transport PDE which represents an aggregate charging dynamics for PEVs depending on the number of grid-connected PEVs and their charging power. It is assumed that the network operator responds to the all grid-connected PEVs through a universal control signal $0 \leq u(t) \leq 1$. Accordingly, each PEV adjusts its charging power through a smart system once it receives the control signal. For extreme cases, the PEVs will be subject to full power charge when $u(t) = 1$ while they will stop charging when $u(t) = 0$.

By integrating the concentration of PEVs $Q(x,t)$ over the energy full storage level $x_{\min} \leq x \leq x_{\max}$ and multiplying it by the instantaneous charging power of PEVs, one can obtain the aggregate charging power of PEVs as

$$P_{\text{demand}}(t) = P_{\max}u(t)\int_{x_{\min}}^{x_{\max}} Q(x,t)dx. \tag{8}$$

In the next section, we will use aggregate power (8) to design a controller for the PDE model (6) to track the reference power trajectory.

III. Control Design Procedure

In this section, we describe the design of a robust control strategy for PDE representation of PEVs aggregate power (6) to track the power supply trajectory $P_{\text{supply}}(t)$. Let us consider the measurable tracking error signal as

$$\begin{aligned} e(t) &= P_{\text{supply}}(t) - P_{\text{demand}}(t) \\ &= P_{\text{supply}}(t) - P_{\max}u(t)\int_{x_{\min}}^{x_{\max}} Q(x,t)dx. \end{aligned} \tag{9}$$

We consider sliding mode theory [9] to design a controller which is robust against the population variations of PEVs. Sliding mode control is a particular type of Variable Structure Control (VSC) that is characterized by a feedback control law and a decision rule known as switching function. In sliding mode control, VSC systems are designed to drive and then constrain the system state to lie within a neighborhood of the switching function. There are two main advantages to this approach. Firstly, the dynamics of the system may be tailored by the particular

choice of switching function. Secondly, the closed-loop response becomes insensitive to uncertainties. The sliding mode design approach consists of two components. The first involves assigning a switching function so that the sliding motion satisfies the design specifications. The second is concerned with the selection of a control law, which will make the switching function attractive to the system state. The following theorem is proposed to control the system described by the PDE model (6) to track the desired reference profile.

Theorem: *For the bilinear PDE dynamics (6), the following control input results in the convergence of the tracking error (5) to zero.*

$$u(t) = u(0) + P_{\max}^{-1} \int_0^t \dot{P}_{\text{supply}}(\tau) \Big[\int_{x_{\min}}^{x_{\max}} Q(x,\tau)dx \Big]^{-1} d\tau + \rho \int_0^t \text{sgn}[e(\tau)]d\tau. \tag{10}$$

Proof: Let us consider $e(t)$ as the sliding manifold and a positive-definite Lyapunov function as

$$V(t) = \frac{1}{2}e^2(t). \tag{11}$$

The time derivative of (11) can be expressed as

$$\dot{V}(t) = e(t) \Big[\dot{P}_{\text{supply}}(t) - P_{\max}\dot{u}(t) \int_{x_{\min}}^{x_{\max}} Q(x,t)dx - P_{\max}u(t) \int_{x_{\min}}^{x_{\max}} \frac{\partial Q(x,t)}{\partial t} dx \Big]. \tag{12}$$

By substituting (6) into (12), the last integral term in (12) can be written as

$$\int_{x_{\min}}^{x_{\max}} \frac{\partial Q(x,t)}{\partial t} dx = - P_{\max}u(t) \int_{x_{\min}}^{x_{\max}} \frac{\partial Q(x,t)}{\partial x} dx + \int_{x_{\min}}^{x_{\max}} \omega(x,t)dx. \tag{13}$$

The first integrand in the right hand of (13) can be rewritten as $dQ(x,t) = \partial Q(x,t)/\partial x dx$. Hence, the corresponding integral in (13) is vanished using the boundary condition (7) and the time-derivative of (11) is obtained by merging (12) and (13) as

$$\dot{V}(t) = e(t) \Big[\dot{P}_{\text{supply}}(t) - P_{\max}\dot{u}(t) \int_{x_{\min}}^{x_{\max}} Q(x,t)dx - P_{\max}u(t) \int_{x_{\min}}^{x_{\max}} \omega(x,t)dx \Big]. \tag{14}$$

Now, by considering the new control input $\nu(t) = \dot{u}(t)$, the aim is to obtain $\nu(t)$ such that the negative-definiteness of (14) is ensured. Let us consider (14) in the following form

$$e(t) \Big[\dot{P}_{\text{supply}}(t) - P_{\max}\nu(t) \int_{x_{\min}}^{x_{\max}} Q(x,t)dx - P_{\max}u(t) \int_{x_{\min}}^{x_{\max}} \omega(x,t)dx \Big] < 0. \tag{15}$$

The control input $\nu(t)$ can be considered as a combination of two control input, namely, equivalent control $\nu_{eq}(t)$ and a discontinuous control $\nu_{dis}(t)$ such that

$$\nu(t) = \nu_{eq}(t) + \nu_{dis}(t). \tag{16}$$

The equivalent control $\nu_{eq}(t)$ is applied to enforce the perturbation-free dynamics (6), i.e., $\omega(x,t) = 0$, to reach the sliding manifold. On the other hand, the discontinuous control $\nu_{dis}(t)$ is applied to keep the system on the sliding manifold and maintain the robustness characteristics against non-zero disturbance, i.e., $\omega(x,t) \neq 0$. By substituting (16) into (15), it can be rewritten as

$$e(t)[\mathcal{P}(t) - \nu_{eq}(t) - \nu_{dis}(t) - \Omega(t)] < 0, \tag{17}$$

where

$$\mathcal{P}(t) = \frac{\dot{P}_{\text{supply}}(t)}{P_{\max} \int_{x_{\min}}^{x_{\max}} Q(x,t)dx}, \Omega(t) = \frac{u(t) \int_{x_{\min}}^{x_{\max}} \omega(x,t)dx}{\int_{x_{\min}}^{x_{\max}} Q(x,t)dx}. \tag{18}$$

It is assumed that $\int_{x_{\min}}^{x_{\max}} Q(x,t)dx > 0$. This implies that the PEVs concentration in the grid never equals zero and there is at least one PEV connected to the grid for charging purpose.

The equivalent control $\nu_{eq}(t)$ can be found from (17) for $\omega(x,t) = 0$ as

$$\nu_{eq}(t) = \mathcal{P}(t) = \frac{\dot{P}_{\text{supply}}(t)}{P_{\max} \int_{x_{\min}}^{x_{\max}} Q(x,t)dx}. \tag{19}$$

Substitution of (19) into (17) results in

$$e(t)[-\nu_{dis}(t) - \Omega(t)] < 0. \tag{20}$$

Now, let the discontinuous control input $\nu_{dis}(t)$ be

$$\nu_{dis}(t) = \rho.\text{sgn}[e(t)], \tag{21}$$

where sgn(.) is the signum function and $\rho > 0$ is a constant that should be determined. During the motion outside the sliding-modes, the switching terms in (21) is liable to cancel the influence of disturbance, and try to make the motion constrained on the switching manifold. Furthermore, substitution of (21) into (20) results in

$$e(t)\{-\rho.\text{sgn}[e(t)] - \Omega(t)\} < 0. \tag{22}$$

The negative definiteness of (22) now can be ensured by choosing $\rho > |\Omega(t)|$. Hence, the sliding mode control input (16) can be expressed in the following form

$$\nu(t) = \frac{\dot{P}_{\text{supply}}(t)}{P_{\max} \int_{x_{\min}}^{x_{\max}} Q(x,t)dx} + \rho.\text{sgn}[e(t)]. \tag{23}$$

Eventually, the control input to the PDE representation of PEVs aggregated power charge (6) can be obtained by integrating the sliding mode control (23)

$$u(t) = u(0) + P_{max}^{-1} \int_0^t \dot{P}_{\text{supply}}(\tau) \Big[\int_{x_{\min}}^{x_{\max}} Q(x,\tau)dx \Big]^{-1} d\tau + \rho \int_0^t \text{sgn}[e(\tau)]d\tau. \tag{24}$$

This completes the proof of the theorem. □

The sliding mode control (24) can be further simplified to

$$u(t) = u(0) + \hat{\rho} \int_0^t \text{sgn}[e(\tau)]d\tau,$$
$$\hat{\rho} > \rho + P_{\max}^{-1} \Big| \int_0^t \dot{P}_{\text{supply}}(\tau) \Big[\int_{x_{\min}}^{x_{\max}} Q(x,\tau)dx \Big]^{-1} d\tau \Big|. \tag{25}$$

The sliding mode control (25) operates upon signum-function or namely switching on the sliding manifold $e(t)$. This characteristics of the sliding mode control, though results in a robust performance of the closed-loop system, may excite the high-frequency dynamics of the system and particularly for broader uncertainty bounds. Such a high-frequency switching is generally referred to as chattering and has been treated via several approaches like boundary layers and sigmoid-like function instead of the signum function. In this paper, we use the saturation function $sat[e(t)/\epsilon] = e(t)/\epsilon$ for $-\epsilon \leq e(t) \leq \epsilon$, $sat[e(t)/\epsilon] = 1$ and -1 for $e(t) > \epsilon$ and $e(t) < -\epsilon$, respectively. Furthermore, the integral term in the control input (25) results in an integrator windup when the control is subject to saturation. To circumvent this problem, we will employ the integrator anti-windup projection operator presented in [1] as

$$u(t) = u(0) + \hat{\rho} \int_0^t \text{Proj}_u\{\text{sgn}[e(\tau)]\}d\tau, \tag{26}$$

where $\text{Proj}_u\{\phi\} = 0$ for $u(t) = 0$ and 1 when $\phi > 0$ and $\phi < 0$, respectively. Otherwise, $\text{Proj}_u\{\phi\} = \phi$.

IV. Monte Carlo Simulation and Discussion

In this section, we present the results of implementing the proposed control scheme based on a Monte Carlo simulation. To obtain a realistic PEV load model and its distribution in the grid, we utilize a daily trip schedule and travel lengths data provided by the National Household Travel Survey (NHTS) [10]. The survey presents a comprehensive data on travel and transportation in the U.S. Application of the realistic NHTS database has been widely sought in the recent vehicle-grid integration [11].

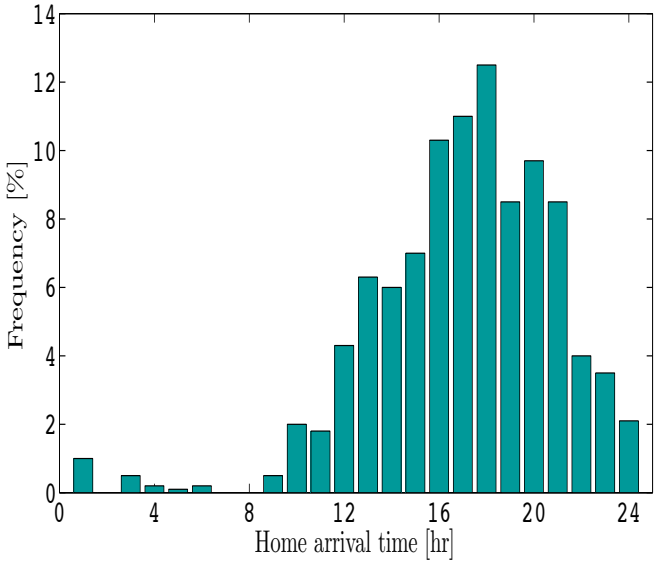

Fig. 1. Home arrival time according to National Household Travel Survey (NHTS)

To create a Monte Carlo simulation, we use a large number of vehicles mapped to the end-of-travel data-set of NHTS as depicted in Fig. 1. It shows the percentage of the vehicles with end of travel time, which indeed is the time that they connect to the grid for charging purpose. For each vehicle, the daily trip energy demand (kWh) is calculated based on the trip length ($Miles$) and the consumption rate of the energy ($Miles/kWh$). Then by assigning a battery size for each vehicle the charging process is started and terminated when: (i) Battery charge meets the daily trip demand, (ii) Battery is charged to its maximum level, or (iii) Battery is plugged out of the grid. To perform the Monte Carlo simulation, the energy consumption rate and effective battery size of PEVs are considered to follow a Gaussian distribution with mean values of $4Miles/kWh$ and $7kWh$, respectively. These values result in an expected trip length of $28Miles$ which is commensurate with the U.S. average daily trip length according to NHTS. To introduce a significant stochasticity into the Monte Carlo simulation, the respective standard deviation for the energy consumption rate and the effective battery size are set to $\%10$ and $\%20$, respectively. It is noted that the control system should be robust enough to deal with the above-described heterogeneous population of the vehicles. Hence, the gain of the controller, $\hat{\rho}$, will be selected sufficiently large to suppress the disturbances caused by incoming/outgoing PEVs and heterogeneity.

In this paper, we use a real wind power data for the reference renewable power provided by the National Renewable Energy Laboratory (NREL) [12]. The data has been collected from a wind farm SW Minnesota within 24 hours. We use 10,000 PEVs with the afore-described specifications and the

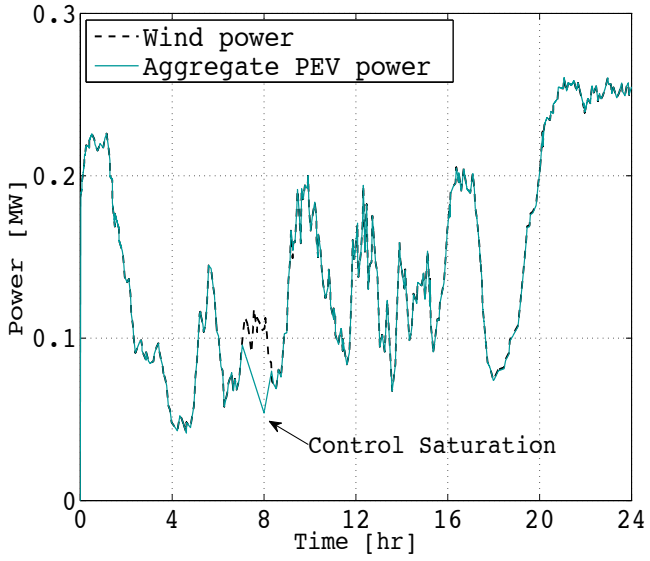

Fig. 2. Wind power tracking response for PEVs with anti-windup integrator

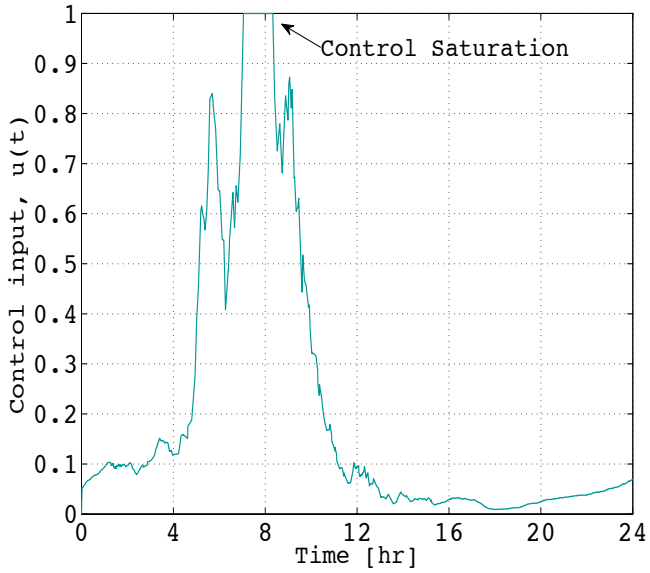

Fig. 4. Control input for PEVs with anti-windup integrator

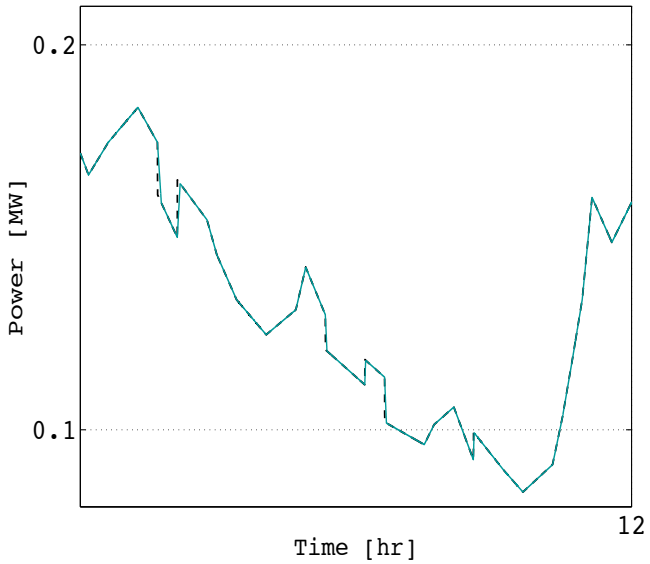

Fig. 3. Tracking performance in a zoomed window for 10AM $\leq t \leq$ 12PM

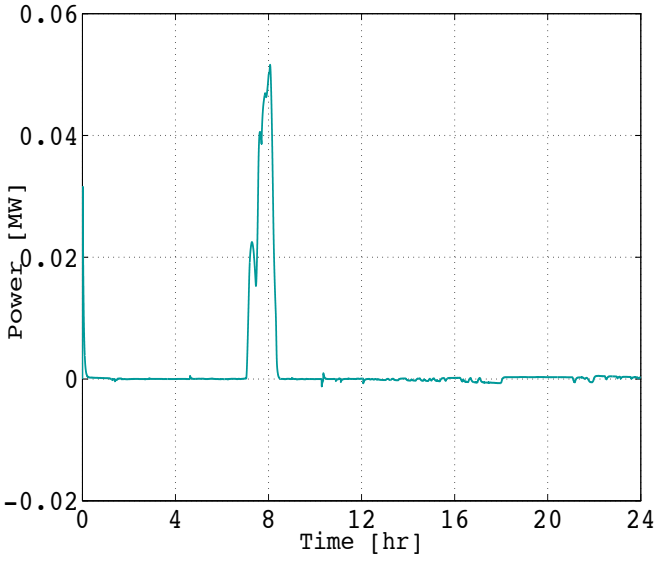

Fig. 5. Tracking error for PEVs with anti-windup integrator

maximum charging power of individual PEVs, $P_{\max} = 2kW$. We will also use MATLAB/Simulink® with Runge–Kutta ODE4 for numerical integration.

Figure 2 demonstrates the aggregate power tracking for the sluggish and intermittent wind power by using the proposed control scheme (25) and the anti-windup operator presented in (26). We have used $\hat{\rho} = 30$ and $\epsilon = 0.1$ for the control gain and boundary layer thickness, respectively. Within the time interval 7AM $\leq t \leq 8:20$AM, where the gird-connected PEVs are minimum (see Fig. 1), the maximum power is transmitted to the PEVs. This inadequacy of PEVs makes the available wind power exceed the demand power by the PEVs. Consequently, the control input reaches its maximum value and saturates until the grid-connected PEVs power demand exceeds the available wind power. The wind power tracking performance has been shown in the zoomed window for 10AM $\leq t \leq$ 12PM in Fig. 3. It shows that the aggregate PEVs power closely tracks the reference wind power. The corresponding control input profile has been depicted in Fig. 4. It can be seen that the controller is able to track the wind power despite severe fluctuation of the wind power. Moreover, it is shown that the control input saturates when the power demand is low because of the fewer number of PEVs connected to the grid during specific time of the day

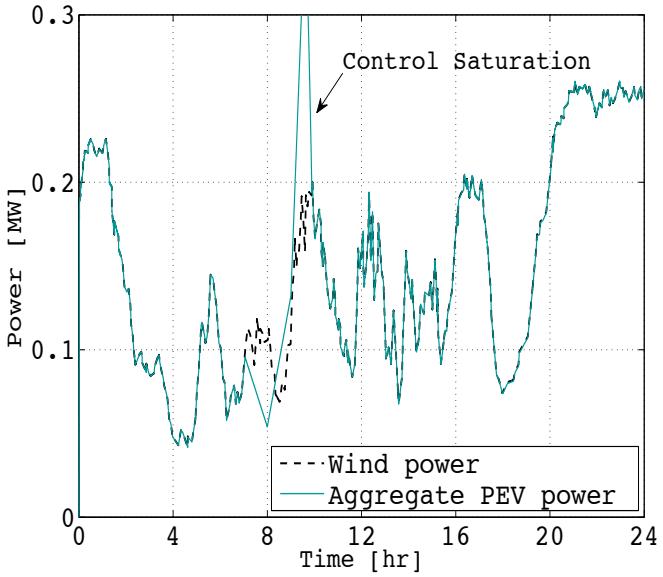

Fig. 6. Wind power tracking response for PEVs without anti-windup integrator

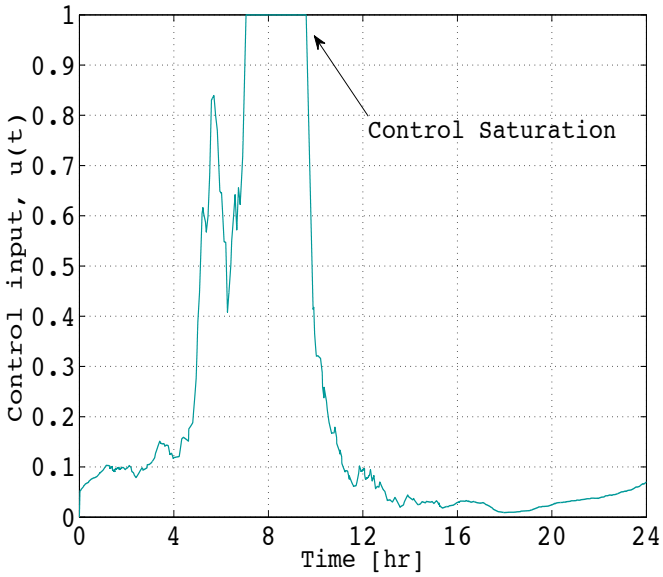

Fig. 7. Control input for PEVs without anti-windup integrator

(7AM $\leq t \leq$ 8 : 20AM). By increasing the number of grid-connected PEVs after 8 : 20AM and demanding more power from the grid, the control input leaves the saturation zone and adjusts the transmitted power to each PEV based on the proposed controller in (25). However, during the control input saturation the tracking error increases drastically and reaches $0.05MW$. The profile of tracking error has been illustrated in Fig. 5.

The preceding simulation results are presented for the proposed controller combined with the integrator anti-windup operator. The anti-windup operator helps to cancel out the integrator windup when the control input is subject to saturation. The results of the closed-loop system without the anti-windup operator has been shown in Fig. 6. It is shown that the reference power tracking is deteriorated when the control input reaches its maximum limit. Due to the windup problem, it takes a longer time for the controller to return back the reference tracking error to zero. The saturation time for the anti-windup case is $\Delta(t) = 1.3hr$ which is considerably less than the corresponding time without the anti-windup operator with $\Delta(t) = 2.6hr$ (see Fig. 7).

V. Conclusion

A systematic approach is proposed in this paper to derive the aggregate charging power of plug-in electric vehicles (PEVs) in the form of a partial differential equation (PDE). The derived PDE is then utilized to design a robust strategy to control the aggregate charging power of PEVs. The proposed controller performance is examined using a Monte Carlo simulation for a large group of grid-connected PEVs in a realistic framework. It was shown that the controller is able to force the aggregate power of the PEVs to track successfully the intermittent and sluggish wind power profile. The integrator windup drawback, which is an intrinsic characteristics of an integral controller due to the zero relative-degree of the system, can lead to a large tracking error when subject to input saturation. To avoid this problem, an anti-windup operator was used to circumvent excessive saturation of the controller.

References

[1] S. Bashash and H. Fathy, Robust demand-side plug-in electric vehicle load control for renewable energy managment, *American Control Conference*, San Francisco, CA, 2011.

[2] H. Lund and W. Kempton, Integration of renewable energy into the transport and electricity sensor through V2G, *Energy Policy*, vol. 36, pp. 3578-3587, 2008.

[3] C. Guille and G. Gross, A conceptual framework for the vehicle-to-grid (V2G) implementation, *Energy Policy*, vol. 37, pp. 4379-4390, 2009.

[4] M. Takagi, K. Yamaji, and H. Yamamato, Power system stabilization by charging power managment of plug-in hybrid electric vehicles with LFC signal, *Vehicle Power and Propulsion Conference*, pp. 822-826, Dearborn, MI, 2009.

[5] D. S. Callaway, Tapping the energy storage potential in electric loads to deliver load following the regulation, with application to wind energy, *Energy Conversion and Managment*, vol. 50, pp. 1389-1400, 2009.

[6] D. S. Callaway and I. A. Hiskens, Achieving controllability of electric loads, *Proceedings of the IEEE*, vol. 99, pp. 184-199, 2011.

[7] S. Bashash and H. Fathy, Transport-based load modeling and sliding mode control of plug-in electric vehicles for robust renewable power tracking, *IEEE Trans. Samrt Grid*, vol. 3, no. 1, pp. 526-534, 2012.

[8] S. Moura, J. Brendtsen, and V. Ruiz, Modeling heterogeneous population of thermostatically controlled loads using diffusion-advection PDEs, *ASME Dynamic Systems and Control Conference*, Palo Alto, CA, 2013

[9] V. I. Utkin, Sliding mode in control and optimazation, Berlin, Springer-Verlag, 1992.

[10] U.S. DOT, National Houshold Travel Survey [http://nhts.ornl.gov].

[11] S. Bashash, S.J. Moura, and H. Fathy, On the aggregate grid load imposed by battery health-concious charging of plug-in hybrid electric vehicles, J. of Power Sources, vol. 196, pp. 8747-8754, 2011.

[12] Yih-Huei Wan, Wind Power Plant Behaviors: Analyses of Long-Term Wind Power Data, NREL/TP-500-36551, Sept. 2004.